Electronic Supplementary Material (ESI) for Dalton Transactions.
This journal is © The Royal Society of Chemistry 2020

Electronic Supporting Information (ESI)

Fast Multipoint Immobilization of Lipase through Chiral L-proline on MOF as Chiral Bioreactor

Stephen Lirio[a‡], Yung-Han Shih[a‡], Pamela Berilyn So,[a] Li-Hao Liu[a], Yun-Ting Yen[a], Shuhei Furukawa[b*], Wan-Ling Liu[c*], Hsi-Ya Huang[a*†] and Chia-Her Lin[d*]

"In memory of Professor Hsi-Ya Huang"

[a]Department of Chemistry, Chung Yuan Christian University, No. 200 Zhongbei Rd., Zhongli District, Taoyuan 32023, Taiwan
[b]Institute for Integrated Cell-Material Sciences (WPI-iCeMS), Kyoto University, Yoshida, Sakyo-ku, Kyoto 606-8501, Japan
[c]College of Science, Chung Yuan Christian University, No. 200 Zhongbei Rd., Zhongli District, Taoyuan 32023, Taiwan
[d]*Department of Chemistry, National Taiwan Normal University, No. 88, Sec. 4, Ting-Chow Rd., Taipei, 11676, Taiwan.*
‡These authors contributed equally
†Deceased August 22, 2017

Table of Contents	
Section S1	Synthesis of MOFs and Experimental procedures
Section S2	Optimization and characterization of the bioreactor
Section S3	Comparison with other literatures
Section S4	Characterization of the aldol product
Section S5	References

Section S1: Synthesis of MOFs and Experimental procedures

Synthesis of MIL-53(Al)

MIL-53(Al) was synthesized according to the published literature.[1] Typically, the synthesis was carried out under hydrothermal conditions using aluminum nitrate nonahydrate ($Al(NO_3)_3 \cdot 9H_2O$), 1,4-benzenedicarboxylic acid (C_6H_4-1,4-$(CO_2H)_2$, H_2BDC), and deionized water. The reaction was performed in a 23 mL Teflon-lined stainless steel hydrothermal bomb under autogenous pressure for three days at 220 °C. The molar composition of the starting mixtures is Al (1.30 g): H_2BDC (0.288 g): H_2O (1:0.5:80). Afterward, the resulting white powdered sample was filtered and washed with deionized water to produce a MIL-53(Al). The MIL-53(Al) was vacuumed and heated at 300 °C for 1 day before further experiments.

Synthesis of DUT-5(Al)

DUT-5 was synthesized according to a modified procedure published earlier.[2] DUT-5 was solvothermally synthesized under microwave-assisted reactions. A mixture of aluminum nitrate nonahydrate ($Al(NO_3)_3 \cdot 9H_2O$: 176 mg, 0.47 mmol), biphenyl-4,4'-dicarboxylic acid ($C_{14}H_{10}O_4$, 97 mg, 0.4 mmol, H_2BPDC), and dimethylformamide (10.0 ml, DMF) was placed in a 100 mL Teflon autoclave placed in a microwave oven. The mixture was heated at 120 °C for 30 min. The resulting white powdered sample was collected by filtration, washed with DMF and dried at room temperature. The DUT-5 was vacuumed and heated at 150 °C for 1 day before further experiments.

Determination of Loading Efficiency

The loading efficiencies of MOFs support for PPL and PPL-Pro were determined using the bicinchoninic acid (BCA) method. Typically, a Cu^{2+}-lipase complex is formed under alkaline condition, followed by the reduction of Cu^{2+} to Cu^{1+} then followed by the formation of the purple-blue complex (BCA-Cu^{1+}) in an alkaline environment. Therefore, the basis of monitoring the reduction of alkaline Cu^{2+} is due to the presence of PPL. Herein, 400 µL of the BCA working reagent (mixing 50 parts of BCA solution (reagent I) with 1 part of Cu^{2+}solution (reagent II)) are mixed with 20 µL of PPL adsorbed supernatant obtained by centrifugation. The loading capacities of PPL@MOFs and PPL-pro@MOFs were calculated based on the absorbance ratio of the residual PPL obtained after immobilization to that obtained by free PPL at the specified concentration. The loading efficiency = $[1-(A_{\text{after immobilization PPL}}/A_{\text{free PPL}})]*100\%$.

Determination of PPL and PPL-Pro activity

The enzyme activities of PPL and PPL-Pro were measured by hydrolysis of p-nitrophenyl palmitate (p-NPP). A 14.4 mM ethanolic p-NPP solution (250 µL) and 50 mM sodium phosphate buffer (pH 7.2) (250 µL) were added to the suspended PPL or PPL-pro. After 5 min reaction, the supernatant was separated by centrifugation (10000 rpm for 5 min). The reaction was terminated upon the addition of 0.5 M Na_2CO_3 (500 µL). The supernatant was diluted 5-folds with D.I. water and determined the absorbance at 405 nm from the hydrolysis product (*p*-nitrophenol) using a UV-Vis spectrometer.

Section S2: Optimization and characterization of the bioreactor

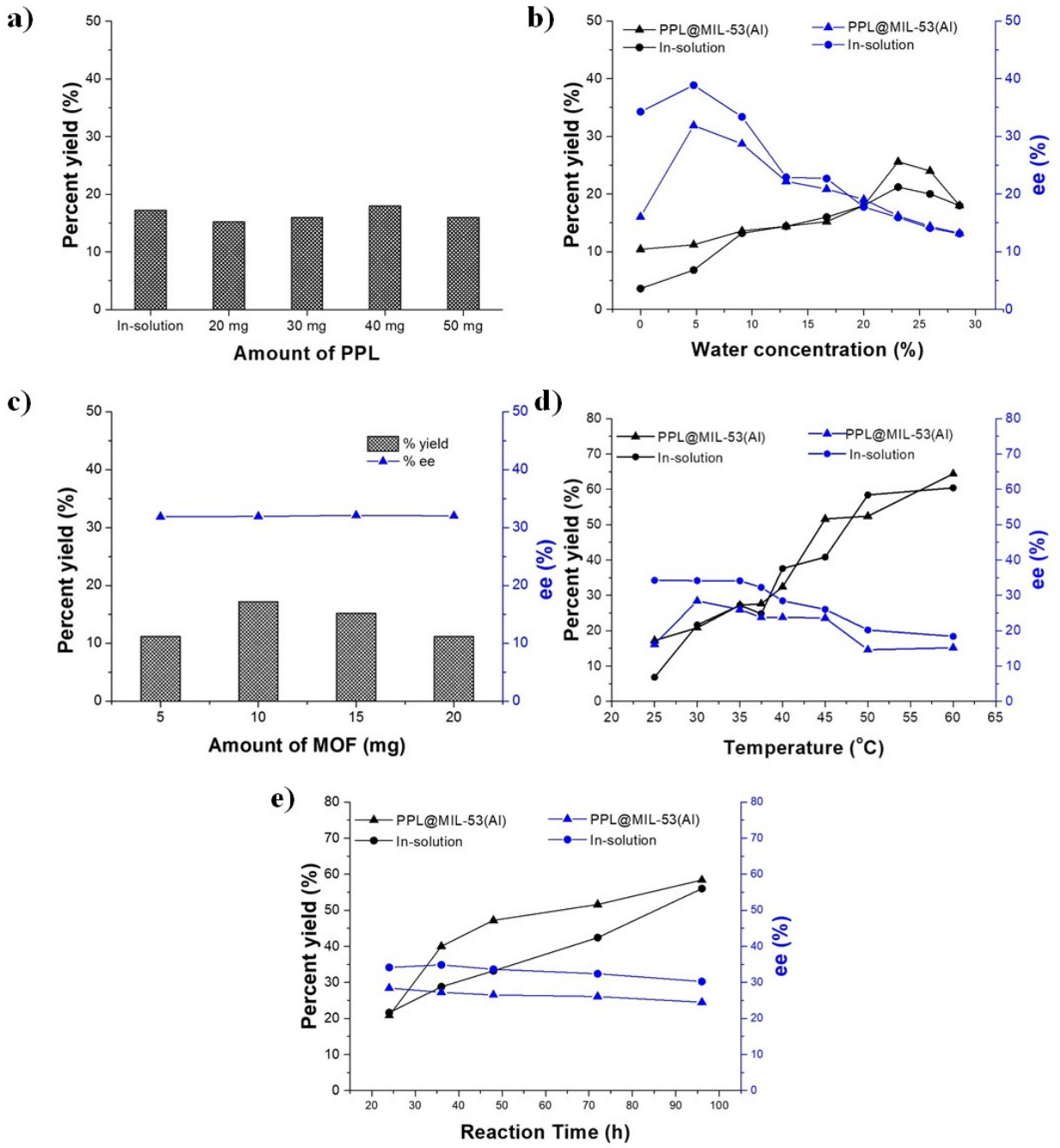

Figure S1. Optimization of parameters affecting catalytic efficiency: Effect of a) amount of PPL, b) water content, c) MOF amount, d) temperature, and e) reaction time on the yield and enantioselectivity for the aldol reaction. The yield and ee were determined by gravity column chromatography and HPLC using the AS-H column, respectively. Conditions are summarized in Table S1.

Table S1. Summary of conditions used in the reactions presented in Figure S1

Figure	4-nitrobenzaldehyde	MIL-53(Al)	PPL	water	acetone	reaction temp.	reaction time
1a	0.125 mmol	10 mg	20-50 mg	125 µL	375 µL	25 °C	24 h
1b		10 mg	40 mg	0-30% water (500 µL total volume)		25 °C	24 h
1c		5-20 mg	40 mg	25 µL	475 µL	25 °C	24 h
1d		10 mg	40 mg	25 µL	475 µL	25-60 °C	24 h
1e		10 mg	40 mg	25 µL	475 µL	25 °C	24-96 h

In Figure S1a, the aldol product increases as the amount of immobilized PPL increases up to 40 mg. However, a further increase of PPL showed a slight decrease in the product yield, suggesting the mass transfer limitation of the substrate[3] and the loading efficiency of the MIL-53. Furthermore, high enzyme loading might change the microenvironment, which is caused by protein aggregation. In Figure S1b, a bell-shaped curve reveals that the concentration of water is significant for aldol reaction. Increasing the water concentration, up to 25%, led to an increase in the product yield but decreases sharply at 30% while the enantioselectivities (ee) sharply declined at lower or higher water concentration. This observation is due to the large excess of water, which decreases the solubility of aldehyde and alters the conformation of the active site of PPL. These results demonstrate that the reaction is sensitive to water concentration, which is in agreement with the previous reports[3, 4]. Therefore, the water content of 5% in the was utilized in the succeeding reactions. In Figure S1c, it can be seen that varying the amount of MOF does not affect the ee, but the highest yield is observed at 10 mg amount. With this, 10 mg of MOF is used for the succeeding optimization. In Figure S1d, the optimum reaction temperature of PPL@MIL-53(Al) was observed at 30 °C. Further increase in the temperature (i.e., 35-70°C) gave higher aldol product, but with low ee. The catalytic efficiency of the immobilized PPL increased with increasing temperature, suggesting that the PPL has higher heat resistance than that of free PPL. Consequently, increasing the temperature highly affects the ee of the product. The bioreactor was further investigated by monitoring the yield and ee as a function of time. As depicted in Figure S1e, the product yield increases as the reaction time progresses up to 60 h (21%-58% yield). However, no significant improvement in the ee was observed despite increasing the reaction time for PPL and PPL@MIL-53. Since the ee was not improved, we selected the 24 h reaction time for the succeeding experiments.

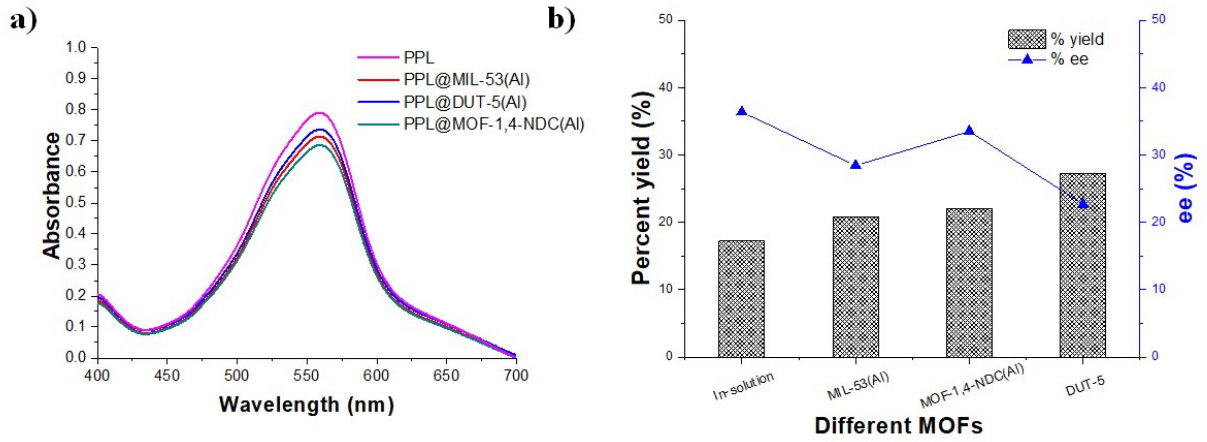

Figure S2. a) Loading efficiency of PPL on different MOFs and b) effect of different MOFs to immobilize the PPL based on the yield and ee of aldol product.

Conditions: 4-nitrobenzaldehyde (0.125 mmol), 10 mg MOF, and PPL (40 mg) in a reaction system containing 475 µL acetone and 25 µL D.I H_2O at 25 °C for 24 h. Calculation for loading efficiency is shown in Page S2. The yield and ee were determined by gravity column chromatography and HPLC using AS-H column, respectively.

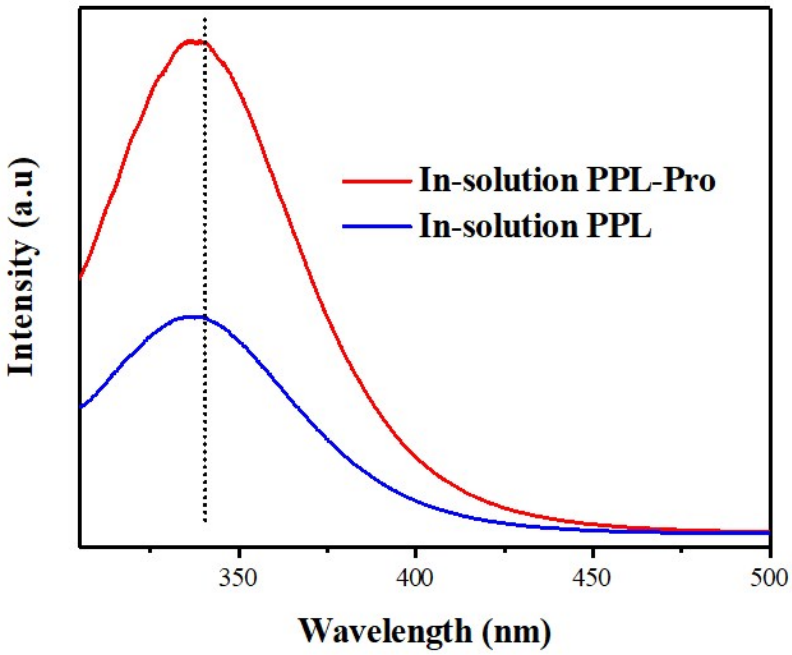

Figure S3. Fluorescence spectra of PPL-pro and PPL. Excitation wavelength: 290 nm. Emission wavelength: 340 nm

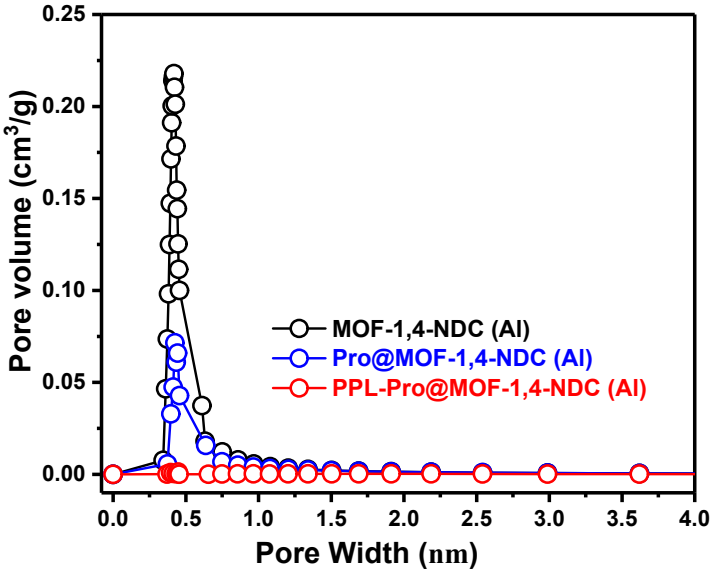

Figure S4: Pore size distribution of pristine MOF-1,4-NDC (Al), Pro@MOF-1,4-NDC (Al) and PPL-Pro @MOF-1,4-NDC.

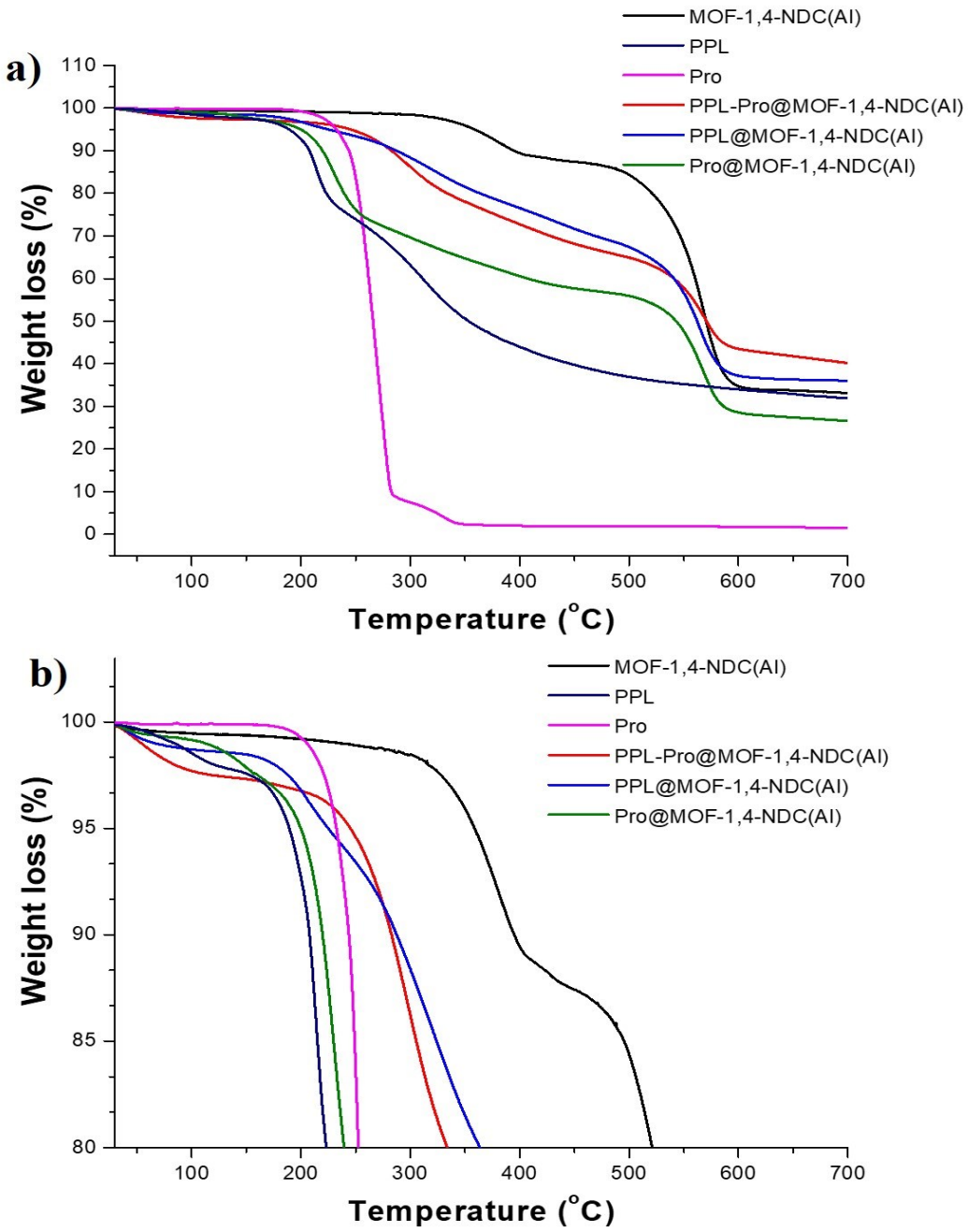

Figure S5: TGA curves of A-B) PPL-Pro@MOF-1,4-NDC, PPL@MOF-1,4-NDC, Pro and pristine MOF-1,4-NDC (full range). Note: B) the scale (y-axis) of TGA curves were adjusted from 80 to 100% weight loss to show the difference of each immobilized catalyst.

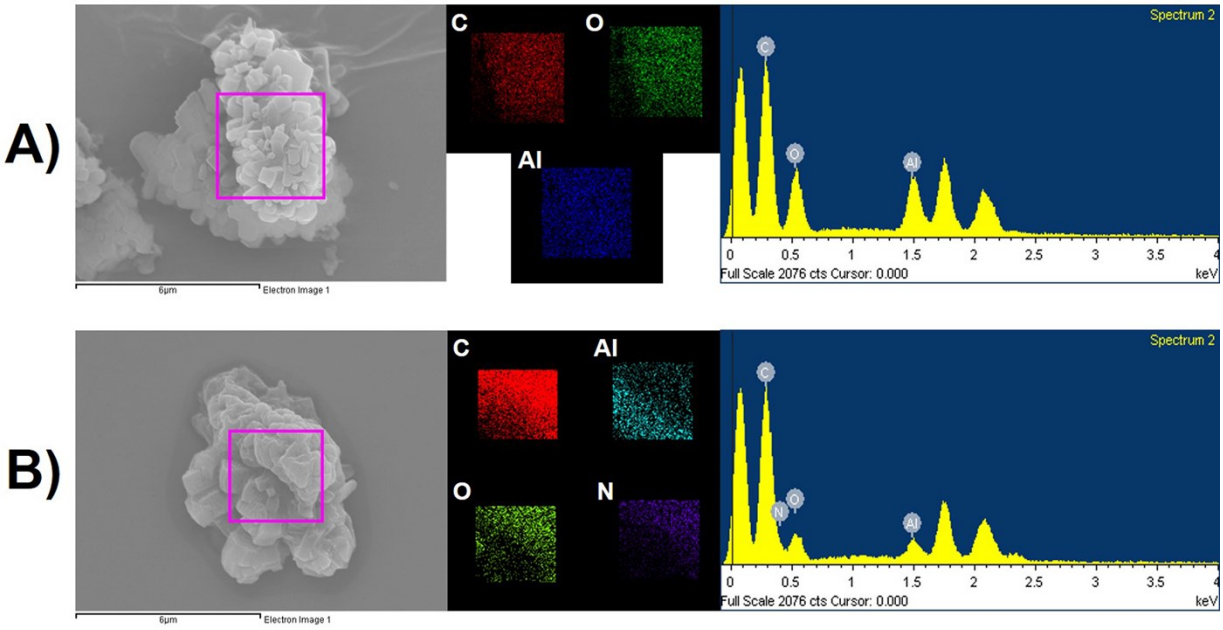

Figure S6: SEM-EDS of A) pristine MOF-1,4-NDC(Al) and B) PPL-Pro@MOF-1,4-NDC(Al).

SEM-EDS analysis of PPL-Pro@MOF-1,4-NDC(Al) (Fig. S11B) shows the existence of carbon, oxygen, aluminum and nitrogen (i.e. from Pro and PPL enzyme) with 49.2%, 18.81%, 3.07% and 28.97%, respectively. The high number of nitrogen content observed in PPL-Pro@MOF-1,4-NDC could be due to overlapping peaks observed between the carbon and nitrogen. Nevertheless, SEM-EDS mapping reveals the existence of dispersed nitrogen throughout the MOF-1,4-NDC, suggesting the successful immobilization of PPL-Pro. To further probe the nitrogen content, elemental analysis was conducted (See Table S2).

Table S2: Elemental analysis of PPL, PPL@MOF-1,4-NDC(Al) and PPL-Pro@MOF-1,4-NDC

Biocatalyst	Carbon (%)	Nitrogen (%)
PPL	43.43	10.17
PPL@MOF-1,4-NDC(Al)	50.62	4.01
PPL-Pro@MOF-1,4-NDC(Al)	53.61	6.32

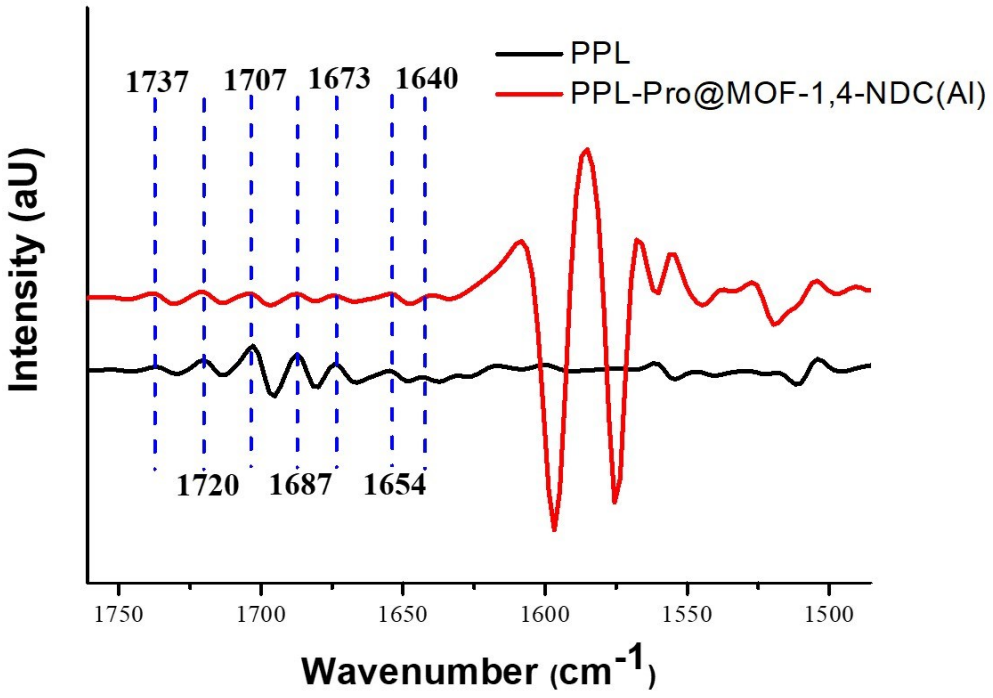

Figure S7: Second derivative FTIR analysis of PPL and PPL-Pro@MOF-1,4-NDC(Al).

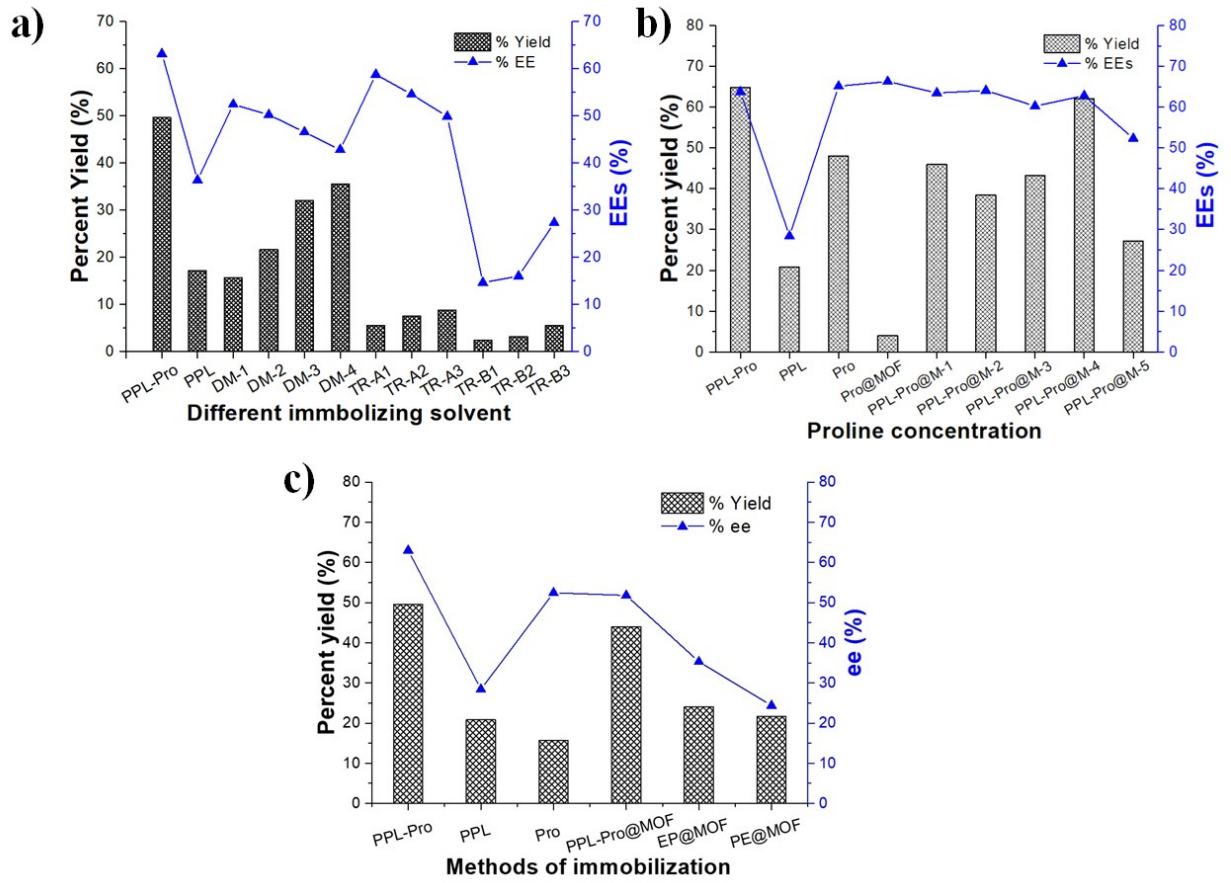

Figure S8: Optimization of catalytic efficiency of PPL-Pro@MOF-1,4-NDC(Al): Effect of a) immobilizing solvent[a], b) proline concentration[b], and c) methods of immobilization[c]. The yield and ee were determined by gravity column chromatography and HPLC using the AS-H column, respectively. Conditions are summarized in Table S3.

[a]DM = DMSO/MeOH (DM-1 to DM-4) is the ratio of the MOF-1,4-NDC:PPL (1:1 to 1:4, MOF-1,4-NDC:PPL); TR-A = Tris Buffer (100 mM) (TR-A1 to TR-A3) is the ratio of MOF-1,4-NDC:PPL (1:1 to 1:3, MOF-1,4-NDC:PPL); TR-B = Tris buffer (25 mM) (TR-B1 to TR-B3) is the ratio of MOF-1,4-NDC:PPL (1:1 to 1:3, MOF-1,4-NDC:PPL). [b]The PPL-Pro@M-1 to PPL-Pro@M-5 = 15% pro increments (i.e. PPL-Pro@M-1 = 15% Pro to PPL-Pro@M-5 = 75% Pro). [c]PPL-Pro@MOF = Pro and PPL were immobilized at the same time. EP@MOF = PPL was first immobilized followed by Pro. PE@MOF = pro was first immobilized followed by PPL.

Table S3. Summary of conditions used in the reactions presented in Figure S8

Figure	4-nitrobenzaldehyde	MOF-1,4-NDC	PPL	Pro	Water/acetone	reaction temp.	reaction time
7a	0.125 mmol	10 mg	10-40 mg	15% mmol	25 µL/ 475 µL	25 °C	24 h
7b			40 mg	15-75% mmol			
7c			40 mg	15% mmol			

Immobilized PPL-Pro (i.e. different PPL at fixed Pro (15% mmol)) on MOF-1,4-NDC(Al) using different immobilizing solvents showed that increasing the amounts of PPL had higher product yield but lower ee (Figure S8a). It was observed that a further increase of PPL caused some aggregation after immobilization and demonstrated a significant effect on the ee. Furthermore, changing the immobilizing solvent to tris-buffer (TR-A, pH 7 (100mM)) at different MOF:PPL ratio afforded low aldol product with decreasing ee as the PPL is further increased (i.e. TR-A1, Figure S8a). The low yield could be ascribed to the low stability of MOF-1,4-NDC(Al) in aqueous solution whereas the positive effect on ee is due to the stability of PPL in buffer solution (TR-A1-A3). Similar results were obtained when low ion concentration of tris-buffer (TR-B, pH 7 (25mM)) was employed to immobilize the PPL-Pro. Therefore, 10 mg of PPL containing 15% mmol of Pro was used to immobilize onto the MOF-1,4-NDC(Al) with the aid of organic solvent rather than buffer solution. The amounts of Pro were also varied at fixed PPL:MOF ratio (1:1). Increasing the amounts of Pro up to 60% enhances both the yield (from 46 to 62%) and ee (63%) but dramatically decreased for 75% mole (27% yield and 52% ee). This result suggests the aggregation of the catalyst, especially when increasing the Pro, up to 75% mole, as it lowers the ee of the aldol product.

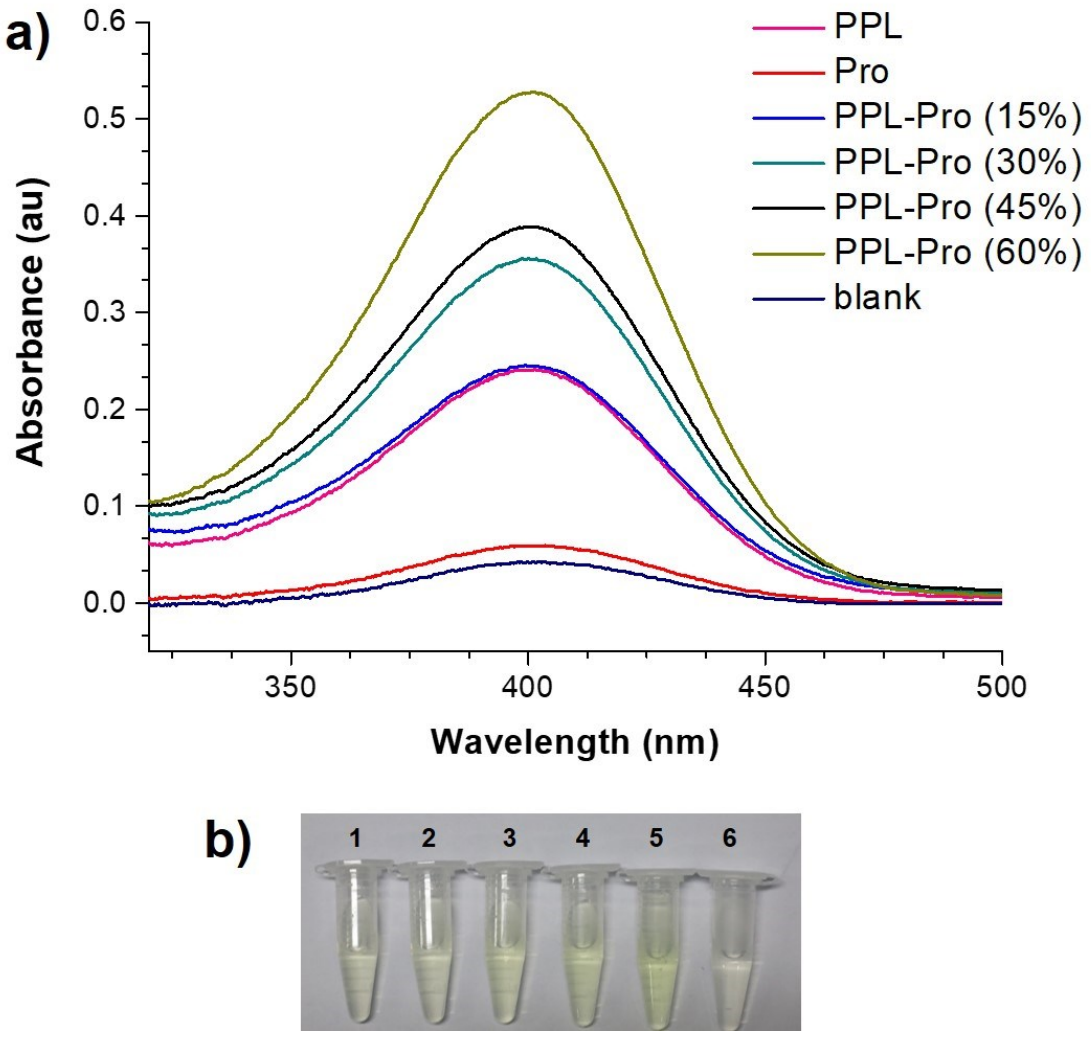

Figure S9: a) UV-vis spectra of PPL, Pro, and PPL-Pro activity at different concentrations of Pro and b) optical images of hydrolyzed *p*-nitrophenyl palmitate (*p*-NPP). (1) PPL only, (2-5) 15% mmol increment of Pro in PPL, and (6) Pro only.

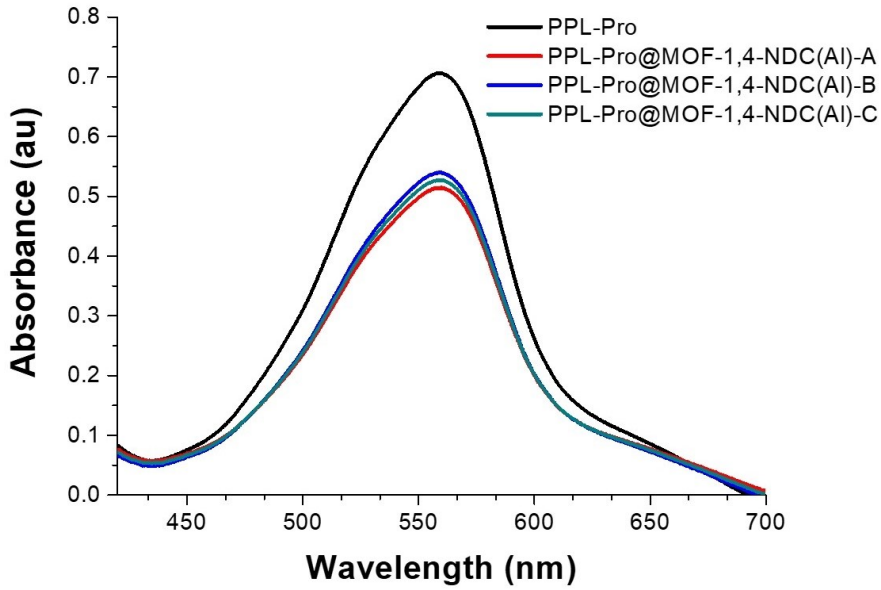

Figure S10: Loading efficiency of different batches of PPL-Pro@MOF-1,4-NDC. The condition and calculation for loading efficiency are shown in Page S2.

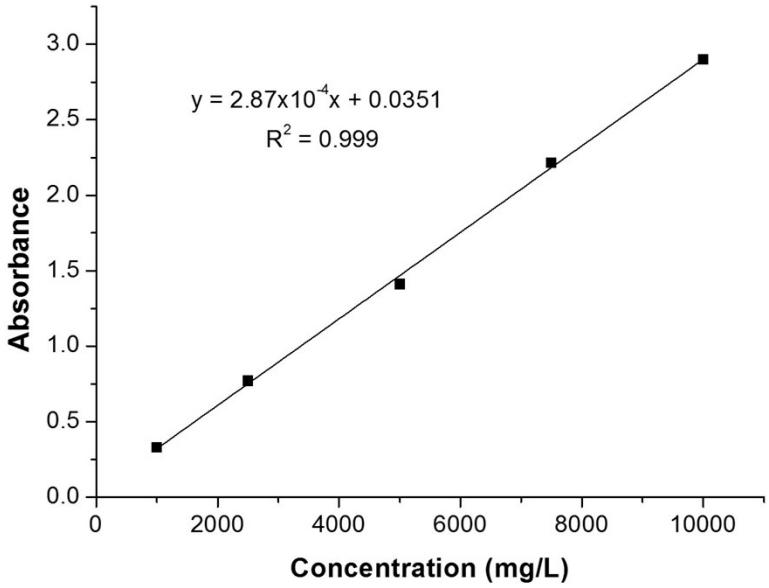

Figure S11: BCA standard calibration curve for loading capacity of MOF-1,4-NDC(Al)

The loading capacity of MOF-1,4-NDC(Al) was calculated based on the obtained equation from the BCA standard curve. The amounts of MOF-1,4-NDC(Al) and PPL used were 10 mg at fixed Pro (6.8 mg) in 1 mL DMSO/Acetone (1:1). After immobilization for 1h, the supernatant was collected. A 40 µL of supernatant was added into a 400 µL BCA solution, heated at 50ºC for 15 mins and cooled down at room temperature for 30 mins. The sample containing the BCA solution was diluted to 1 mL using D.I H_2O and analyzed using a UV-Vis spectrophotometer at 560 nm. The absorbance of the supernatant (i.e unimmobilized) PPL was found to be 2.071. The loading capacity of MOF-1,4-NDC(Al) was determined to be 0.291 mg PPL/mg carrier.

Table S4. Catalytic effect of PPL enzyme, Pro on the product yield and enantioselectivity.

Catalyst	% Yield	% ee
BSA[a]	<1 [a]	2
BSA[a] + D-Pro	53	-63[b]
BSA + L-Pro	49	40
PPL + L-Pro	65	64
PPL + D-Pro	43	-50[b]

[a]BSA = Bovine serum albumin; [b]S-form

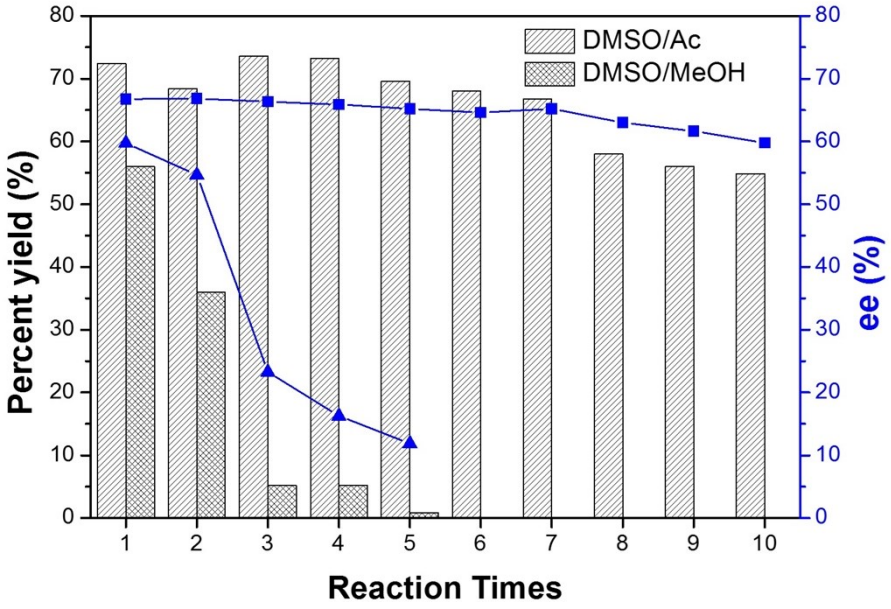

Figure S12: Effect of the immobilizing solvent on the recyclability of PPL-Pro@MOF-1,4-NDC(Al).

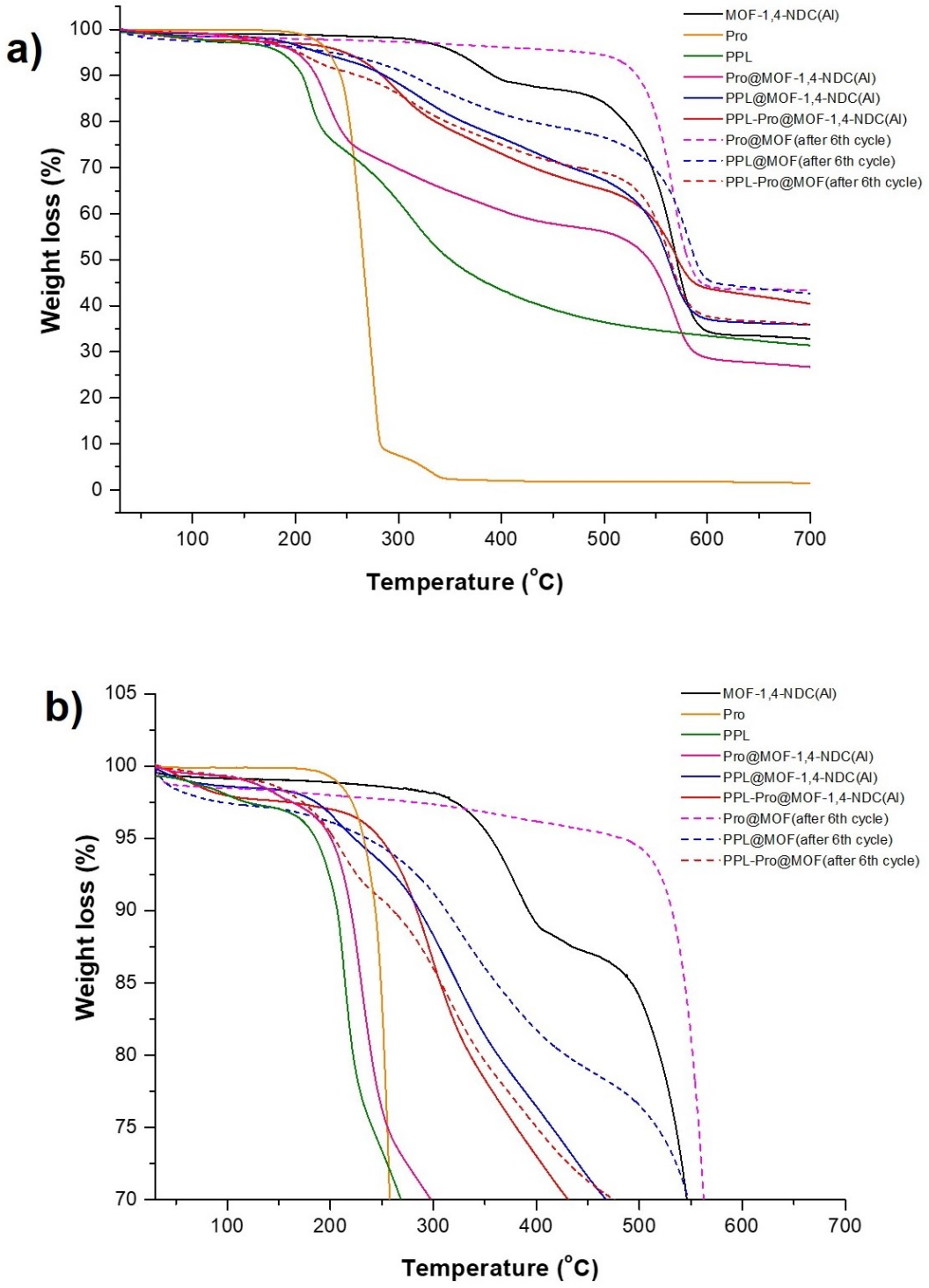

Figure S13. TGA curves of a) PPL-Pro@MOF-1,4-NDC(Al), Pro@MOF-1,4-NDC(Al) and PPL@MOF-1,4-NDC(Al) before and after 6th catalytic cycles. Note: b) the scale (y-axis) for TGA curves were adjusted from 70 to 100% weight loss to show the difference of each immobilized catalyst before and after 6th catalytic cycles.

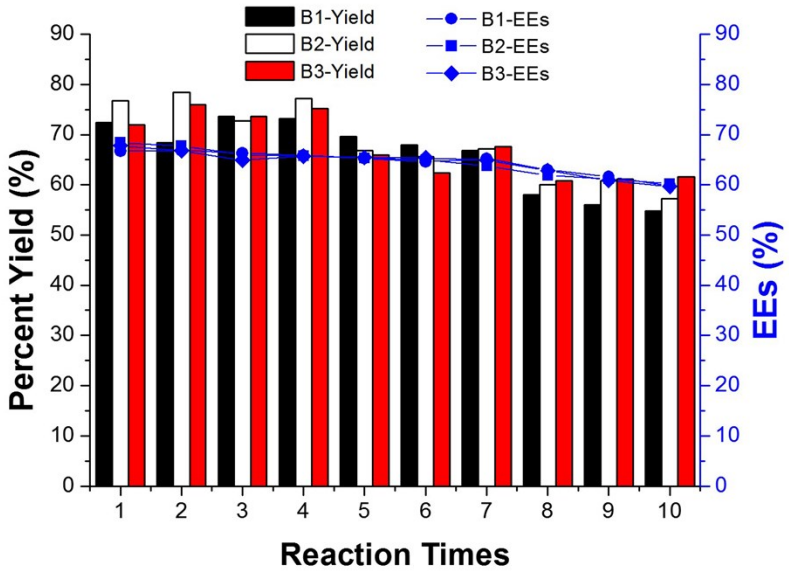

Figure S14: The yield and ee of the aldol product using different batches of PPL-Pro@MOF-1,4-NDC(Al). Conditions: 4-nitrobenzaldehyde (0.125 mmol), 10 mg MOF-1,4-NDC, Pro (6.8 mg, 60% mmol) and PPL (10 mg) in a reaction system containing 475 µL acetone and 25 µL D.I H_2O at 25ºC for 24 h. The yield and ee were determined by gravity column chromatography and HPLC using the AS-H column, respectively. (B1 to B3 = Batch 1 to 3).

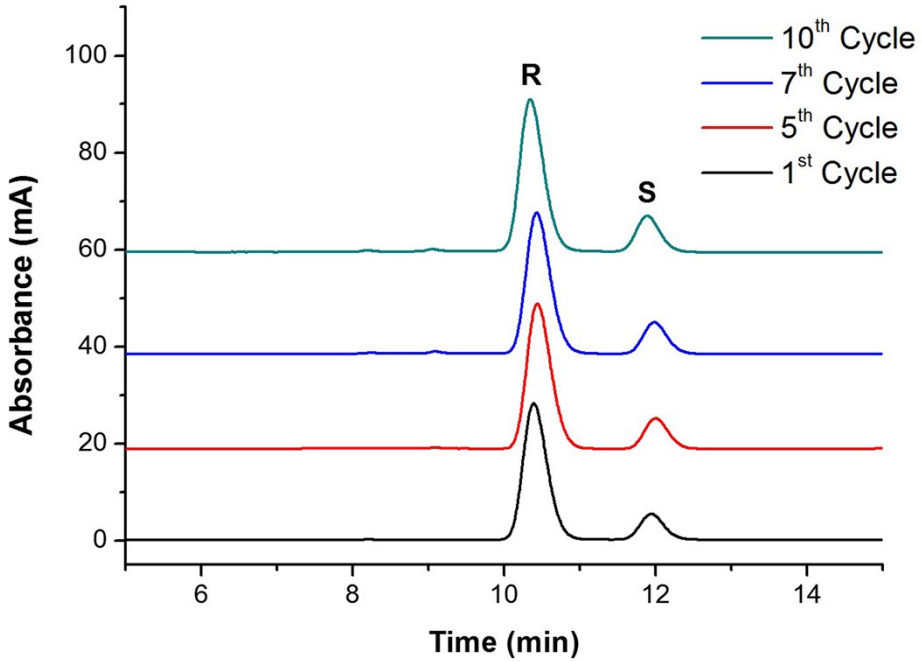

Figure S15: HPLC chromatogram of R-4-hydroxy-4-(4'-nitrophenyl)-2-butanone at several catalytic cycles. The enantiomeric excess was determined by HPLC (Daicel Chiralpak AS-H, *i*-PrOH/hexane= 40:60), UV 254 nm, flow rate of 1.0 mL/min. *R*-isomer, t_R 12.55 min and *S*-isomer, t_R 12.27 min.

Section S3: Comparison with other literatures

Table S4: Comparison with literature using different MOFs to catalyze aldol reactions.

Catalyst	Substrate	Type of Modification (Time, h)	Reaction Time	Yield (%)	% EE (%)	Reused Time	Reference
Zn-MOF[a]	Aldehyde and cyclohexanone	PSM[b] (72 h)	168 h	< 76	< 70	-	[5]
Al-MIL-101-NH-Gly-Pro[c]	*p*-nitro-benzaldehyde and acetone	PSM[b] (0.5 h)	168 h	< 95	< 27	-	[6]
Ap@3[d]	*p*-nitro-benzaldehyde and acetone	PSM[e] (48 h)	48 h	<77	<80	3	[7]
UiO-68-NHPro	p-nitro-benzaldehyde and cyclohexanone	Thermal treatment (96 h)	240 h	<97	<76	3	[8]
PPL-Pro@MOF-1,4-NDC	*p*-nitro- benzaldehyde and acetone	Vortex mixture (1 h)	24 h	< 75[f]	< 70[f]	10	This study

[a] MOF (Zn-DPYI) and chiral azide (L or D-2-azidomethylpyrrolidine) as substrates for the click reaction,[b] PSM = post modification [c] Al-MIL-101-NH-Gly-Pro: Gly = glycine and Pro = proline, [d] (S)-2-(dimethylaminomethyl) pyrrolidine entrapped by $[Zn_4O]_{2/3}[Zn_7L_2(H_2L)_2(OH)_2]\cdot 3H_2O$, [e] solution adsorption in THF at 0 °C, [f] Batch-to-batch MOF-1,4-NDC (n=3).

Table S5: Comparison with literature using different promiscuous enzyme-catalyzed aldol reactions.[a]

Enzyme	Reaction Time	Yield (%)	% EE (%)	Reused Time	Reference
Lipase	168 h	96.4	14.7	-	[4]
APE1547[b]	170 h	71.2	70.1[c]	-	[9]
Pepsin	96 h	54	44	-	[10]
Alcalase-CLEA[d]	48 h	84	12	-	[11]
Trypsin[e]	46 h	28	16	-	[12]
Chymopapain	120 h	12	14	-	[13]
PPL-Pro@MOF-1,4-NDC(Al)	24 h	< 75[f]	< 70[f]	10	This study

[a] Model compound: 4-nitrobenzaldehyde and acetone, [b] APE 1547 = recombinant hyperthermophilic esterase from *Aeropyrum pernix* K1, [c] S form, [d] Immobilized Protease from *Bacillus licheniformis* (commercially available), [e] Trypsin from porcine pancreas, [f] Batch-to-batch MOF-1,4-NDC (n=3)

Section S4: Characterization of the aldol product

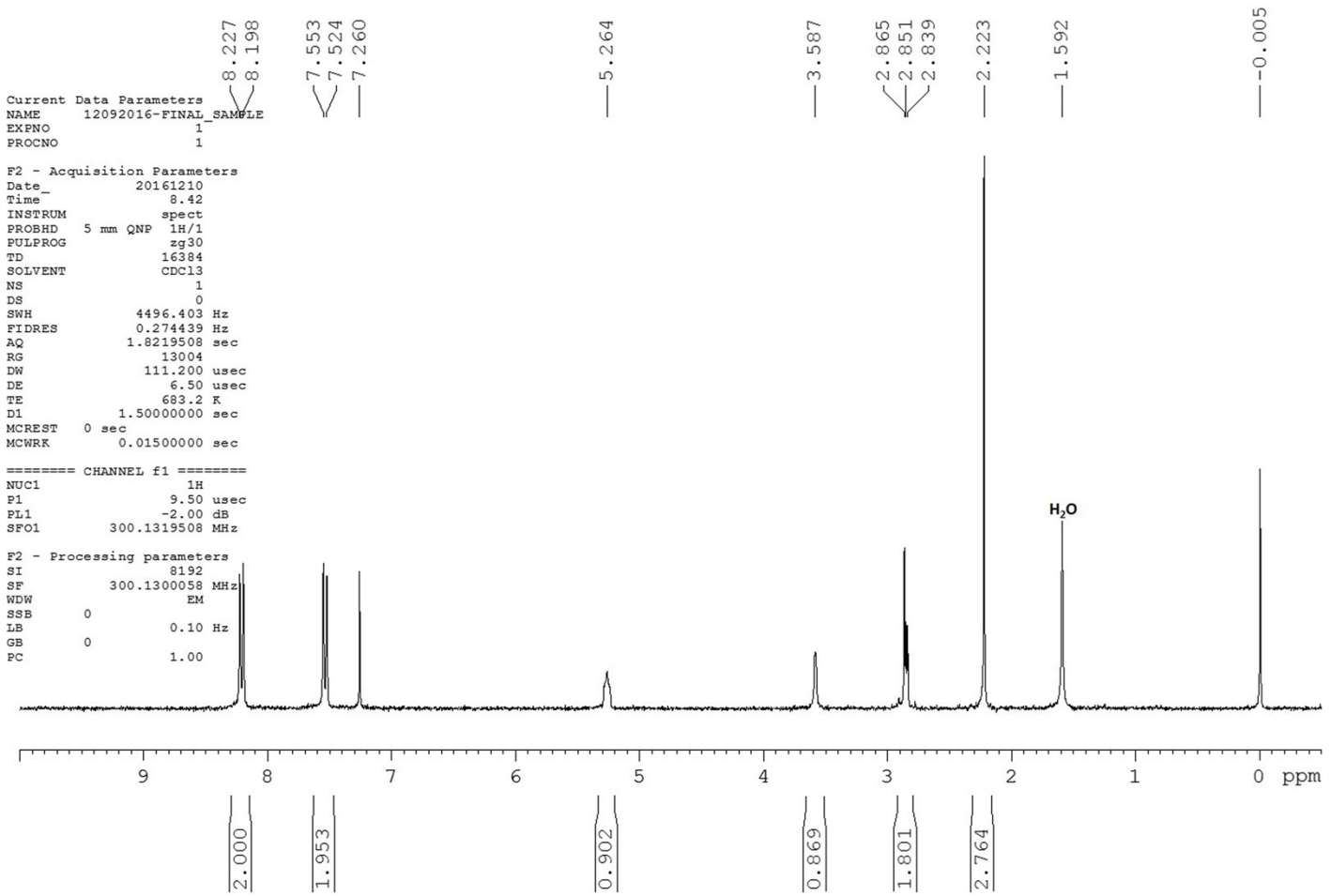

Figure S16. ^{1}H-NMR Spectra of 4-hydroxy-(4'-nitrophenyl)-2-butanone

^{1}H-NMR (300 MHz, $CDCl_3$) δ_H (ppm) = 2.22 (s, 3H), 2.85 (m, 2H), 3.58 (bs, 1H), 5.26 (dd, 1H), 7.54 (d, 2H), 8.21 (d, 2H).

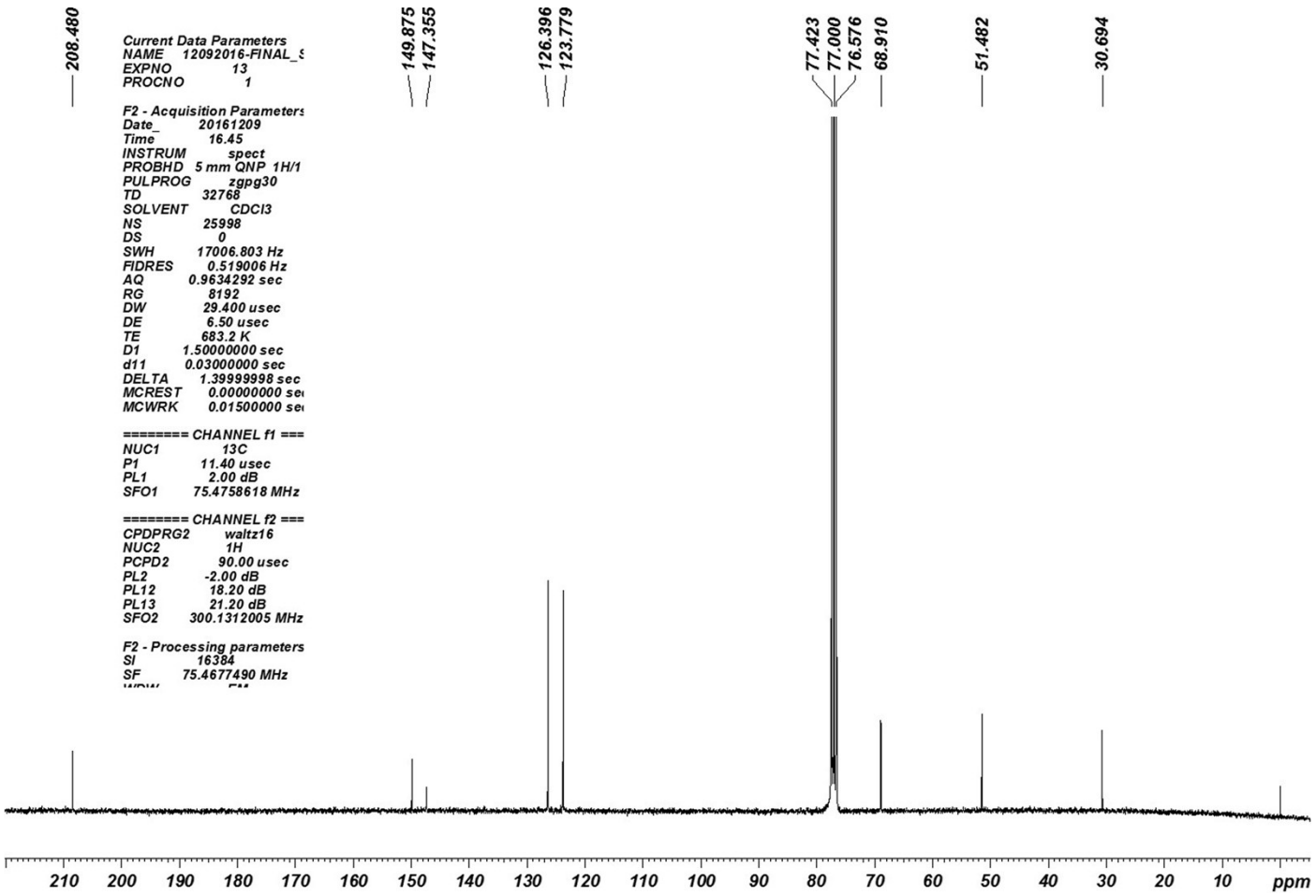

Figure S17. ^{13}C-NMR Spectra of 4-hydroxy-(4'-nitrophenyl)-2-butanone

^{13}C-NMR (300 MHz, $CDCl_3$) δ_C (ppm) = 30.69, 51.48, 68.91, 123.78, 126.40, 147.355, 149.875, 208.84.

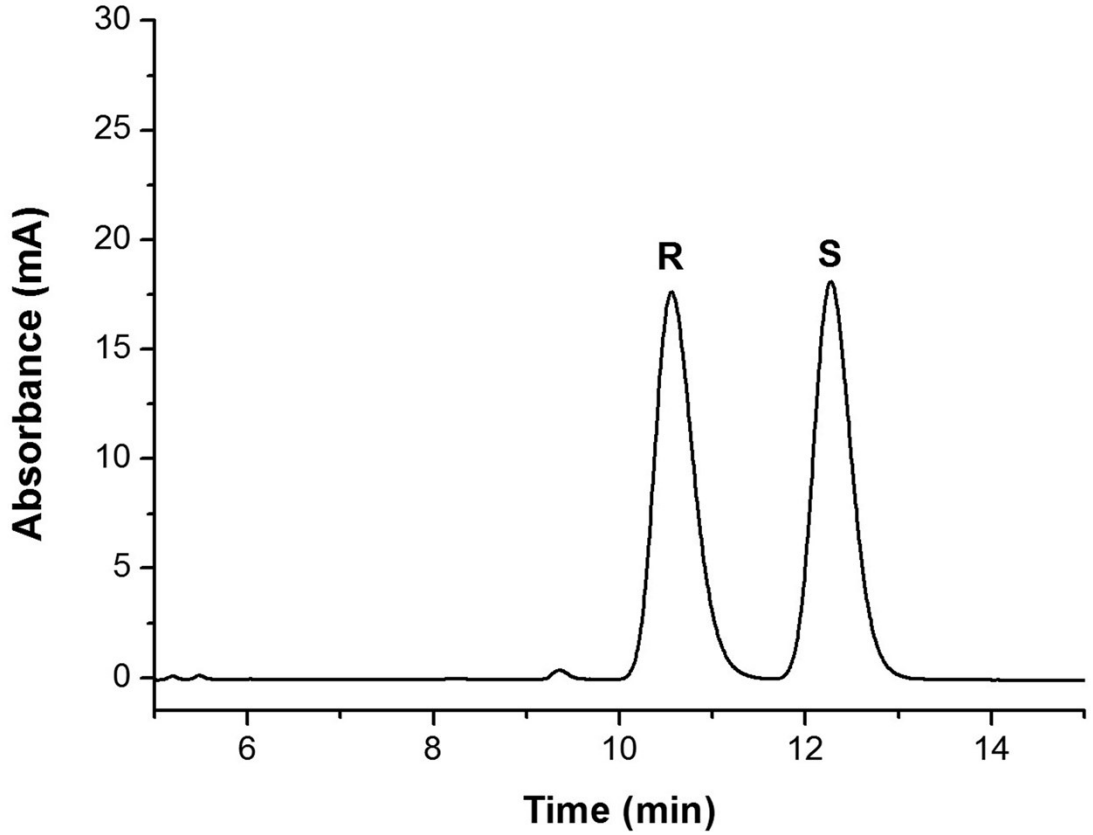

Figure S18. HPLC chromatogram of racemic 4-hydroxy-(4'-nitrophenyl)-2-butanone.
Enantiomeric excess was determined by HPLC (Daicel Chiralpak AS-H, *i*- PrOH/hexane= 40:60), UV 254 nm, flow rate 1.0 ml/min. *R*-isomer, t_R 12.55 min and *S*-isomer, t_R 12.27 min.

Section S5: References

1. T. Loiseau, C. Serre, C. Huguenard, G. Fink, F. Taulelle, M. Henry, T. Bataille and G. Férey, *Chemistry – A European Journal*, 2004, **10**, 1373-1382.
2. I. Senkovska, F. Hoffmann, M. Fröba, J. Getzschmann, W. Böhlmann and S. Kaskel, *Microporous and Mesoporous Materials*, 2009, **122**, 93-98.
3. Z.-B. Xie, N. Wang, L.-H. Zhou, F. Wan, T. He, Z.-G. Le and X.-Q. Yu, *ChemCatChem*, 2013, **5**, 1935-1940.
4. C. Li, X.-W. Feng, N. Wang, Y.-J. Zhou and X.-Q. Yu, *Green Chem.*, 2008, **10**, 616-618.
5. W. Zhu, C. He, P. Wu, X. Wu and C. Duan, *Dalton Transactions*, 2012, **41**, 3072-3077.
6. J. Bonnefoy, A. Legrand, E. A. Quadrelli, J. Canivet and D. Farrusseng, *Journal of the American Chemical Society*, 2015, **137**, 9409-9416.
7. Y. Liu, X. Xi, C. Ye, T. Gong, Z. Yang and Y. Cui, *Angew. Chem. Int. Ed.*, 2014, **53**, 13821-13825.
8. C. Kutzscher, G. Nickerl, I. Senkovska, V. Bon and S. Kaskel, *Chem. Mater.*, 2016, **28**, 2573-2580.
9. W. Haoran, W. Zhi, Z. Hong, C. Ge, Y. Hong and W. Lei, *Green Chemistry Letters and Reviews*, 2014, **7**, 145-149.
10. C. Li, Y.-J. Zhou, N. Wang, X.-W. Feng, K. Li and X.-Q. Yu, *Journal of Biotechnology*, 2010, **150**, 539-545.
11. M. López-Iglesias, E. Busto, V. Gotor and V. Gotor-Fernández, *Advanced Synthesis & Catalysis*, 2011, **353**, 2345-2353.
12. Y.-L. Chen, W. Li, Y. Liu, Z. Guan and Y.-H. He, *Journal of Molecular Catalysis B: Enzymatic*, 2013, **87**, 83-87.
13. Y. Xue, L.-P. Li, Y.-H. He and Z. Guan, *Sci. Rep.*, 2012, **2**, 761.